analytical chemistry

Article

pubs.acs.org/ac

Self-Assembled DNA Hydrogel as Switchable Material for Aptamer-Based Fluorescent Detection of Protein

Lei Zhang, Jianping Lei,* Lin Liu, Changfeng Li, and Huangxian Ju

State Key Laboratory of Analytical Chemistry for Life Science, School of Chemistry and Chemical Engineering, Nanjing University, Nanjing 210093, People's Republic of China

Supporting Information

ABSTRACT: The methodology based on target-responsive structural switching is powerful in bioanalysis with the controllability and sensitivity. In this paper, an aptamer-functionalized DNA hydrogel was designed as a specifically target-responsive switchable material for protein detection. This pure DNA hydrogel was constructed by using a Y-shaped DNA and an aptamer linker through a DNA self-assembly without synthetic polymer backbone. With use of thrombin as the model analyte, the DNA hydrogel was first applied to visual detection with the entrapped Au nanoparticles (AuNPs) as indicating agent. Furthermore, the positively charged quantum dots (QDs) as the fluorophore were synthesized by using polyethyleneimine (PEI) as wrapper and characterized with spectroscopy, transmission electron micrograph, ζ potential, and dynamic laser scattering techniques. Along with a gel-to-sol transition in the presence of the target, the released negatively charged AuNPs from the hydrogel could approach the positively charged QDs. Due to the electrostatic interaction, fluorescence resonance energy transfer between PEI-QDs and AuNPs therefore occurred and quenched the fluorescence signal for the sensitive detection of thrombin. This assay for the detection of thrombin showed a good linear relationship in a range of 0.075 to 12.5 μM with a detection limit of 67 nM at 3σ, and demonstrated excellent feasibility in complex serum matrixes. The biocompatible DNA hydrogel provides a universal switchable material for signal transduction and significantly demonstrates proof-of-concept for the detection of proteins.

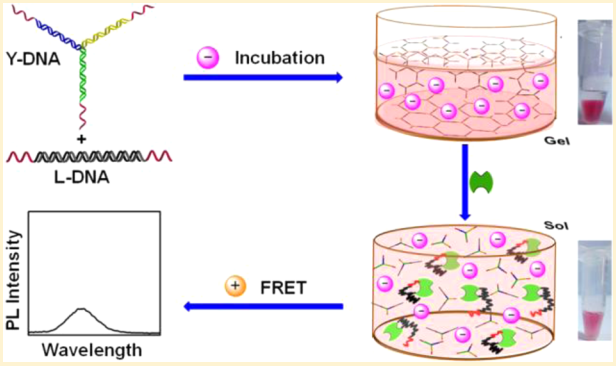

Hydrogels have been widely used as stimuli responsive materials in various applications including controlled drug and gene release systems, sensors, and tissue engineering[1−5] because their networks are sensitive to many stimuli such as temperature, pH, light, and molecular recognition.[6−9] It is therefore interesting to link stimuli responsive hydrogels to DNA that exhibits various functions.[10−16] In particular, aptamer-functionalized hydrogels have elegantly been applied in bioanalysis due to excellent molecular recognition properties.[17−21] For example, an adenosine-responsive hydrogel was first achieved with the polyacrylamide chain as the backbone for controllable release of encapsulated molecules or nanomaterials and drugs.[19] More recently, a glucoamylase-trapped aptamer-cross-linked hydrogel was constructed with a personal glucose meter for the development of a portable system for quantitative detection of nonglucose targets.[21] Although these polymer hydrogel-based methods show the good performance in bioassays, the requirements of laborious modification steps for DNA−polymer hybrids limit their practical applications. Considering that DNA itself is a natural polymer, DNA alone hydrogels without synthetic polymers could be prepared through DNA ligase,[22,23] intermolecular i-motif structures,[24] and DNA hybridization.[25] It is desirable to develop easy and fast strategies by DNA alone hydrogels for applications to biosensing. In this work, an aptamer-functionalized DNA alone hydrogel as target responsive material was prepared for protein detection by incorporating inorganic nanomaterials including gold nanoparticles (AuNPs) and quantum dots (QDs) as signal indicators.

Semiconductor QDs have unique photophysical properties that offer significant advantages for fluorescent bioanalysis.[26] In particular, QDs-based fluorescence resonance energy transfer (FRET) has been regarded widely as an extremely useful tool for the sensitive determination of biomolecules.[27,28] Compared with organic dyes that usually suffer from photobleaching,[29] AuNPs as the acceptors open new perspectives to detect biomolecules owing to their strong FRET quenching efficiency.[30,31] Typically, an inhibition-assay method for the sensitive detection of the protein avidin was proposed through the modulation of FRET efficiency between biomolecule-conjugated QDs and AuNPs.[32] Most of the conjugations between QDs and AuNPs are based on the biological or chemical couplings, such as streptavidin−biotin,[32] β-cyclodextrin−protein,[33] and amide reaction,[34] which usually demand complex modification processes and cost much time. Here, by

Received: August 31, 2013
Accepted: October 18, 2013
Published: October 18, 2013

   dx.doi.org/10.1021/ac4027725 | *Anal. Chem.* 2013, 85, 11077−11082

Scheme 1. Schematic Representation of Self-Assembled DNA Hydrogel As a Switchable Material for Colorimetric and Fluorescent Detection of Thrombin

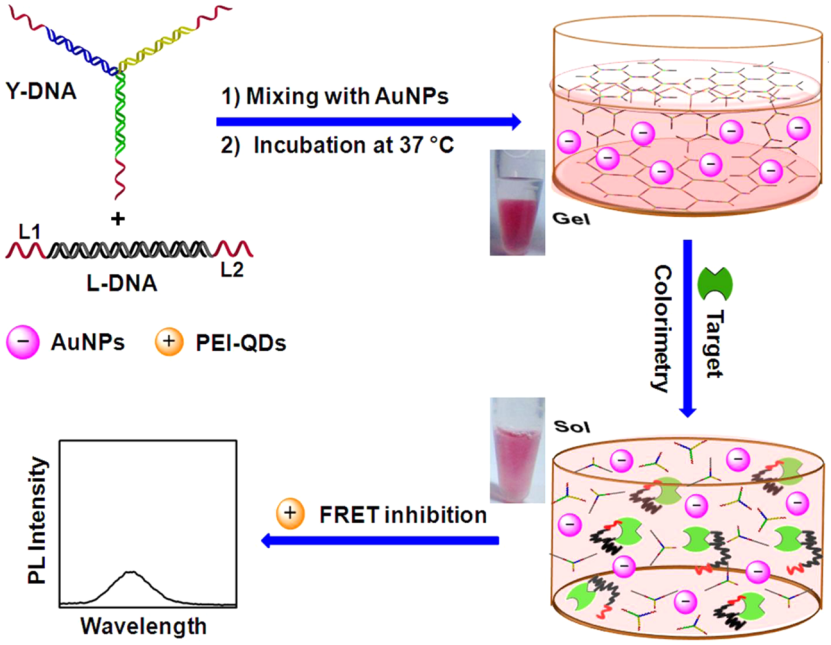

integrating with a target-responsive switchable DNA hydrogel, a FRET inhibition strategy was achieved through electrostatic interaction between positively charged QDs and negativly charged AuNPs for the detection of thrombin.

Thrombin is an important serine protease in serum. For the efficient detection of thrombin, an aptamer-functionalized DNA hydrogel was designed as a target-responsive switchable material from gel to solution (Scheme 1). The DNA hydrogel was directly assembled by two building blocks: Y-shaped DNA (Y-DNA) and linker DNA (L-DNA) composed of an aptamer sequence (L1) with two different recognition sites (APT15 and APT 29)[35] for thrombin and the complementary sequence (L2). Since the "stick ends" in the Y-DNA and L-DNA were complementary to each other, the DNA hydrogel was formed by the cross-linking hybridization between Y-DNA and L-DNA. The rigid space formed in DNA hydrogel could encapsulate AuNPs with diameters of only a few nanometers. When adding the buffer to the hydrogel, two layers would be observed with a colorless upper solution and a red lower layer of AuNP-containing gel in the absence of the target. Upon adding thrombin, it will competitively bind with the L-DNA aptamer, leading to the collapse and dissolution of the DNA hydrogel. Thus the AuNPs were released from the gel to the upper solution for visual detection. Furthermore, based on the FRET between positively charged polyethyleneimine (PEI)-functionalized QDs and negatively charged AuNPs, a fluorescence quenching strategy was developed for the sensitive detection of thrombin in complex matrixes. The biocompatible DNA hydrogel as a switchable material provides an avenue for constructing a biosensing platform for in vivo applications.

EXPERIMENTAL SECTION

Materials and Reagents. Mercaptopropionic acid (MPA), bovine serum albumin, and thrombin were obtained from Sigma-Aldrich. Cadmium chloride ($CdCl_2 \cdot 2.5H_2O$), tellurium powder, and polyethyleneimine (PEI, branched, MW 1,200, 99%) were purchased from Alfa Aesar China Ltd. Chloroauric acid ($HAuCl_4 \cdot 4H_2O$) and trisodium citrate were obtained from Shanghai Reagent Co. Ltd. (Shanghai, China). Sodium borohydride was purchased from Tianjin Chemagent Research Co., Ltd. UltraPower nucleic acid dye was purchased from BioTeke Corporation (Beijing, China). Ultrapure water obtained from a Millipore water purification system (≥18 MΩ, Milli-Q, Millipore) was used in all assays. A buffer consisting of 20 mM Tris-HCl (pH 7.4), 100 mM NaCl, 5 mM KCl, 1 mM $CaCl_2$, 1 mM $MgCl_2$, and 8.5% glycerol (v/v) was used to dissolve thrombin. DNA oligonucleotides were synthesized and purified by Sangon Biological Engineering Technology & Co. Ltd. (Shanghai, China) and stored in Tris-HCl solution (10 mM, pH 8.0) containing 1 mM ethylenediaminetetraacetic acid (EDTA) and 50 mM NaCl. The sequences of these designed oligonucleotides according to eight empirical rules[36] were as follows:

Y1: CACGGACTTGGATCCGCATAACCATTCGCCG-TAATG

Y2: CACGGACTCATTACGGCGAATGTACCGAAT-CAGCCT

Y3: CACGGACTAGGCTGATTCGGTAGTTATGCG-GATCCA

L1: AGTCCGTGGTAGGGCAGGTTGGGGTGACTG-GTTGGTGTGGTTGG

L2: AGTCCGTGCCAACCACACCAACCAGTCACCC-CAACCTGCCCTAC

Here, L1 was a DNA strand composed of two thrombin-binding aptamers, APT 29 and APT 15.

Apparatus. Fluorescence measurements were conducted on a RF-5301PC fluorescence spectrometer (Shimadzu Co., Japan). UV−vis absorption spectra were obtained with a UV-3600 UV−vis−NIR spectrophotometer (Shimadzu Co., Kyoto, Japan) and Nanodrop-2000C nanophotometer (Thermo Scientific, USA). The transmission electron micrograph (TEM) was obtained by using a JEM-2100 TEM instrument (JEOL, Japan). ζ potential measurements were carried out in a Zetasizer Nano-Z Zeta Potential Analyzer (Malvern Instru-

dx.doi.org/10.1021/ac4027725 | Anal. Chem. 2013, 85, 11077−11082

ments Ltd., England). Dynamic light scattering (DLS) measurements were performed by BI-200SM light scattering apparatus (Brookhaven Instruments Co., U.S.A.) equipped with a digital correlator at 640 nm.

Preparation of Y-DNA and L-DNA. In a typical experiment, isometric amounts of DNA strands of Y-DNA (Y1, Y2, and Y3) and L-DNA (L1 and L2) were individually added to the annealing buffer for DNA (10 mM Tris-HCl, pH 8.0, 1 mM EDTA, and 50 mM NaCl) to give a final concentration of 20 μM for each DNA strand. The resulting mixtures were heated to 95 °C for 5 min, and subsequently cooled to room temperature for 2 h to form the designed structures.

Preparation of AuNPs-Entrapped DNA Hydrogel. To form the desired DNA hydrogel, the mixture of Y-DNA and L-DNA with a final concentration of 0.5 and 0.75 mM, respectively, was heated to 95 °C for 5 min and cooled to room temperature for 2 h. To introduce AuNPs in the hydrogel, citrate-modified AuNPs were mixed with the building blocks prior to the gelling process, which was enabled by the cross-linking hybridization between Y-DNA and L-DNA. The mixtures were incubated at 37 °C for 3 h. After washing with buffer to remove gel surface-bound AuNPs, the gel was placed in a Tris-HCl buffer.

Preparation of AuNPs, MPA-QDs, and PEI-QDs. AuNPs stabilized with citrate were synthesized according to the literature procedure.[37] MPA-QDs were prepared in aqueous solution according to the previous reports.[38,39] Typically, freshly prepared NaHTe solution was added to the N_2-saturated $CdCl_2$ solution at pH 9.0 in the presence of MPA as a stabilizing agent. The molar ratio of Cd^{2+}/stabilizer/NaHTe was fixed at 4:10:1. The resulting mixture was then subjected to heating at 110 °C for 6.5 h to control the CdTe nanocrystals with the fluorescent emission at 535 nm. Before usage, the as-prepared QDs solution was purified and sedimentated in 1:1 (v/v) isopropyl alcohol/water and centrifuged at 10 000 rcf for 30 min. The precipitation was then dissolved in deionized water. PEI-QDs were synthesized by mixing the prepared MPA-CdTe QDs solution with 1 mg mL^{-1} PEI in ultrapure water through electrostatic interactions. The suspension was stirred overnight at room temperature and the resultant mixture was centrifuged, then washed twice with deionized water to obtain the PEI-functionalized QDs with good biocompatibility.

Gel Electrophoresis. The 12% native polyacrylamide gel electrophoresis (PAGE) was prepared by using 1×Tris-Borate-EDTA (TBE) buffer. The loading sample was mixed with 7 μL of DNA sample, 1.5 μL 6×loading buffer, and 1.5 μL UltraPower· dye, and kept for 3 min so that the dye can integrate with DNA completely. Then the loading sample was applied onto the lane. The gel was run at 90 V for 90 min in 1×TBE buffer, then scanned using a Molecular Imager Gel Doc XR (BIO-RAD, USA).

Fluorescence Analysis. With the gel-to-sol transition, a specified amount of the upper solution of the DNA hydrogel was added in the PEI-QDs solution. In this work, 200 μL of the final solution was used for the fluorescence measurement. The fluorescence spectra were obtained by scanning from 450 to 650 nm at an excited wavelength of 350 nm equipped with a xenon lamp. The slit width was 5 nm.

RESULTS AND DISCUSSION

Preparation of DNA Hydrogel. To construct DNA hydrogel, the building blocks of Y-DNA and L-DNA were first prepared and verified by PAGE (Figure 1A). Compared with the fast migration of three single-stranded DNAs

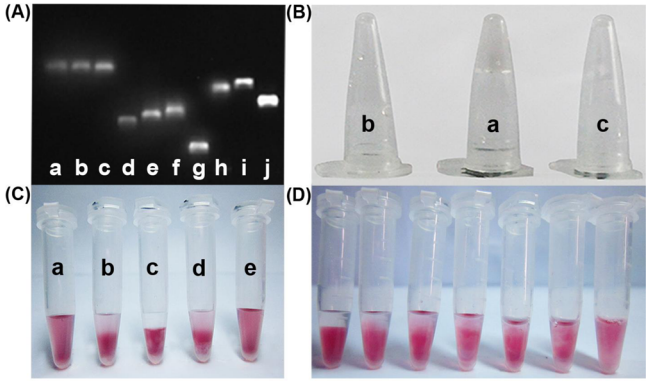

Figure 1. (A) PAGE analysis of Y1 (a), Y2 (b), Y3 (c), Y1 + Y2 (d), Y1 + Y3 (e), Y2 + Y3 (f), Y1 + Y2 + Y3 (g), L1 (h), L2 (i), and L1 + L2 (j). (B) Photograph of self-assembled DNA hydrogel (a) assembled by 0.5 mmol L^{-1} Y-DNA (b) and 0.75 mmol L^{-1} L-DNA (c). (C) DNA hydrogels with different molar ratios of Y-DNA/L-DNA at 1:3 (a), 1:2 (b), 1:1.5 (c), 1:1 (d), and 2:1 (e). AuNPs were trapped in the DNA hydrogel with a cover layer of 20 mM Tris-HCl buffer. (D) Photograph of assembled DNA hydrogels responding to thrombin at the concentration of 0, 1, 5, 10, 50, 100, and 500 μM (from left to right), respectively.

(ssDNAs) in Y-DNA (lanes a, b, and c), the two-component mixture individually showed one band at shorter electrophoresis distance (lanes d, e, and f), indicating the occurrence of partial hybridization among three DNA strands. After the three ssDNAs were mixed at the molar ratio of 1:1:1, a band with slowest migration rate was observed, suggesting the formation of self-assembled Y-DNA (lane g). Similarly, L-DNA (lane j) demonstrated a shorter electrophoresis distance than that of each strand (lanes h and i). Moreover, the dominant single bands of lanes g and j indicated that the assembling processes of Y-DNA and L-DNA were efficient. Subsequently, the DNA hydrogel was successfully synthesized by assembly of Y-DNA with L-DNA (Figure 1B). Compared with the solutions of building blocks (photos b and c), the gel still remained at the bottom of the container, indicating the loss of its fluidity (photo a). To help visualize the gelling formation and transition, AuNPs were employed as indicating agents. Before being utilized, AuNPs were modified with bovine serum albumin (BSA) to avoid aggregation in a high salt concentration DNA buffer.

To obtain a stable hydrogel, the influence of two building blocks was investigated at different molar ratios of 1:3, 1:2, 1:1.5, 1:1, and 2:1 (Figure 1C). At molar ratios of 1:3 and 2:1, the red appearance in upper buffer solutions indirectly suggested no formation of stable hydrogel due to the relative minority for one of the building blocks. In contrast, at the molar ratios of 1:2, 1:1.5, and 1:1, the hydrogel was formed with the colorless upper solution and the red AuNP-containing gel in the lower layer. Obviously, the self-assembled DNA hydrogel at the molar ratio of 1 Y-DNA:1.5 L-DNA was a stable structure for the trapping of AuNPs, and there was no release of AuNPs after several days without stirring or heating.

Visual Analysis of Thrombin. Upon the strong affinity between the aptamer and the thrombin target, the DNA hydrogel would collapse and dissolve in the presence of thrombin. In this way, the AuNPs were released into the upper

dx.doi.org/10.1021/ac4027725 | Anal. Chem. 2013, 85, 11077−11082

solution, facilitating a visual detection method of thrombin. The optimized DNA hydrogel with entrapped AuNPs was investigated for the visual response to different concentrations of thrombin (Figure 1D). The gel tended to disassemble to solution as the concentration of target increased, which is consistent with the increase in absorbance at approximately 520 nm from UV−vis spectra (Figure S1A, Supporting Information). The calibration plot showed a linear relationship between the relative absorbance and the logarithmic value of the concentration of thrombin from 1 to 100 μM (Figure S1B, Supporting Information). The low concentration for visual detection of the present hydrogel may be attributed to the stimuli-sensitive structure of self-assembled DNA and two recognition sites of aptamers for thrombin.

Characterization of AuNPs, MPA-QDs, and PEI-QDs. The TEM image showed that the diameter of the obtained AuNPs was ∼13 nm with the surface plasmon absorption at 520 nm (Figure S2, Supporting Information). The MPA-stabilized CdTe nanocrystals (MPA-QDs) were synthesized by hydrothermal method with a clear UV−vis absorption at 500 nm (Figure 2A, curve a) and a strong fluorescent emission peak

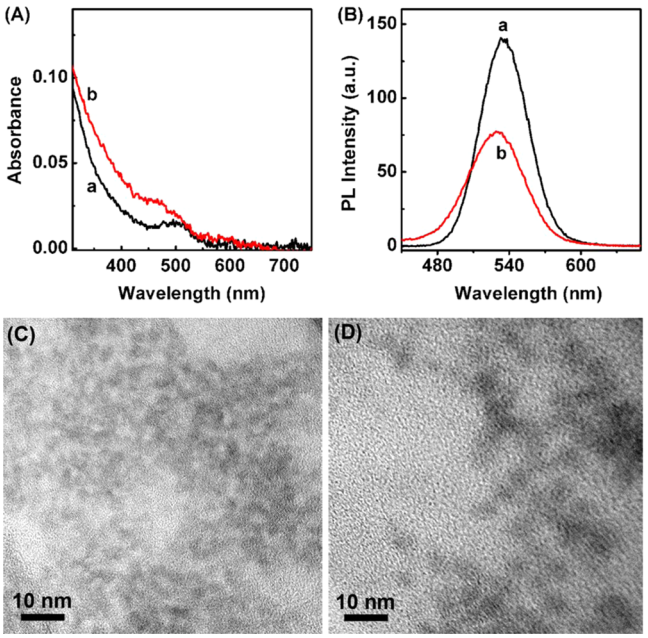

Figure 2. (A) UV−vis and (B) fluorescence spectra of MPA-QDs (a) and PEI-QDs (b). TEM images of (C) MPA-QDs and (D) PEI-QDs.

at 535 nm (Figure 2B, curve a). After being modified with PEI, a positively charged polymer, the absorption peak of PEI-QDs displayed a blue shift to 474 nm (Figure 2A, curve b), correspondingly, the fluorescent emission wavelength showed a slight movement from 535 to 530 nm (Figure 2B, curve b), suggesting the change of QDs surface state. According to Peng's empirical quation,[40] the concentration of the redispersed PEI-QDs solution was estimated to be ∼22 nM.

TEM images further verified the successful functionalization of QDs with PEI. The typical TEM image of MPA-CdTe QDs showed a uniform size distribution of 3−4 nm (Figure 2C). After functionalized with PEI, the TEM image became blurry and a large size of 5−8 nm was observed (Figure 2D). Distribution of the hydrodynamic diameter for MPA-QDs and PEI-QDs in aqueous suspension was also measured by dynamic light scattering. The average hydrodynamic diameter of QDs and PEI-QDs was 5.1 and 9.5 nm, respectively (Figure S3, Supporting Information), which was essentially in agreement with TEM results. In addition, ζ potential distribution clearly proved the change of surface-charge for MPA-QDs and PEI-QDs, because the ζ potential of the former was −28.4 mV and that of the latter was +54.1 mV (Figure S4, Supporting Information). The positively charged PEI-QDs provided for the possibility of FRET with the released negatively charged AuNPs via electrostatic interaction.

FRET between PEI-QDs and AuNPs. UV−vis spectroscopy is usually limited due to the low sensitivity compared with photoluminescence (PL). For more sensitive detection, FRET assay was employed in this DNA hydrogel system. PEI-QDs were used as the donor because the PL emission spectrum has great overlap with the absorption spectrum of AuNPs (Figures 2B and S2, Supporting Information). The negatively charged MPA-QDs led to little fluorescence quenching due to the repulsive interaction between MPA-QDs and AuNPs (Figure 3A), while PL of PEI-QDs was obviously quenched in the

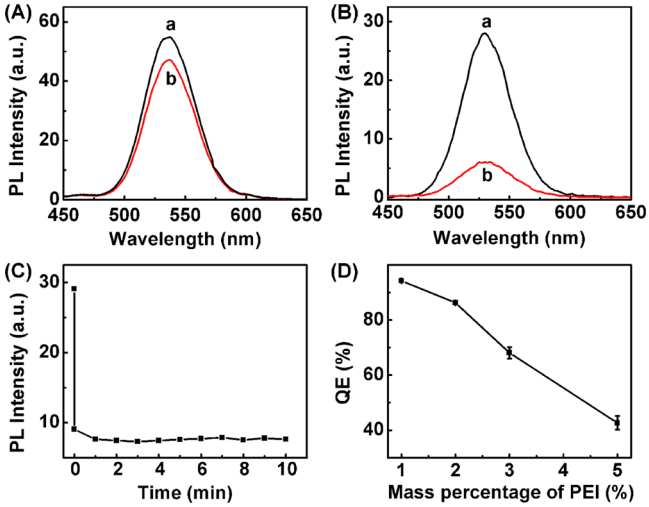

Figure 3. Fluorescence spectra of (A) MPA-QDs and (B) PEI-QDs in the absence (a) and the presence (b) of AuNPs. (C) Fluorescence quenching of PEI-QDs by AuNPs as a function of time. Fluorescence intensity was recorded at 530 nm with an excitation wavelength of 350 nm. (D) Fluorescence QE of PEI-QDs modified with different amounts of PEI in the presence of AuNPs.

presence of AuNPs (Figure 3B), indicating that the electrostatic interaction between the oppositely charged PEI-QDs and AuNPs is responsible for the process of FRET. Upon addition of AuNPs, the fluorescence intensity of PEI-QDs reduced rapidly to 20% of the original intensity in 1 min (Figure 3C). This fluorescence quenching could be ascribed to the energy transfer from PEI-QD to AuNPs via electrostatic interaction, as in the case of the FRET inhibition between persistent luminescence nanoparticles and AuNPs.[41] To further testify the FRET process, PL changes of PEI-QDs with the addition of AuNPs were investigated at different mass percentages of PEI (Figure 3D). Since a high concentration of PEI would lead to a long distance between QDs and AuNPs, and block this FRET process, a lower fluorescence quenching efficiency (QE) was obtained with the increasing of mass percentages of PEI, suggesting that the fluorescence quenching mainly contributed to FRET.

dx.doi.org/10.1021/ac4027725 | Anal. Chem. 2013, 85, 11077−11082

Optimization of Detection Conditions. The effect of the initial amount of gold loaded in hydrogel was investigated on the sensitivity of this method (Figure S5, Supporting Information). With an increasing amount of AuNPs loaded in hydrogel, PL of PEI-QDs was quenched to a higher degree in the presence of the thrombin target. Meanwhile, the DNA hydrogel could not be formed when larger amounts of AuNPs were incorporated into hydrogel. Therefore, 40 μL of 12 nM AuNPs was chosen in this work.

The percentage of BSA that protected AuNPs and incubation time between thrombin and DNA hydrogel were important factors in fluorescent detection of thrombin. A higher FRET efficiency was obtained as the percentage of BSA decreased from 1% to 0.05% (Figure 4A). However, between 0.05% and

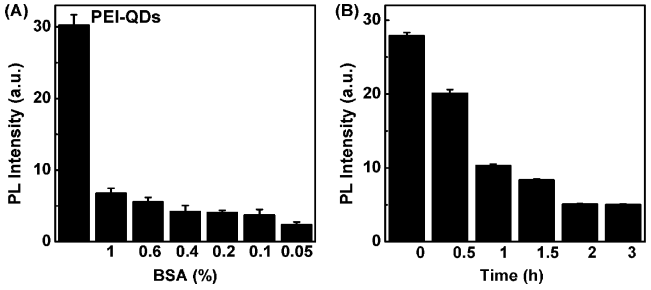

Figure 4. Dependence of PL intensity of PEI-QDs on (A) different amounts of BSA (0.05% to 1%) protected AuNPs and (B) incubation time between self-assembled DNA hydrogel and thrombin.

0.1% BSA, AuNP-modified BSA aggregated a little in the DNA hydrogel. Thus 0.2% BSA was used for the modification of AuNPs due to the good stability and acceptable FRET efficiency.

The incubation time between thrombin and the aptamer was also crucial in the gel-to-sol transition. At 37 °C, the hydrogel gradually disassembled as the incubation time increased, leading to the release of AuNPs from DNA hydrogel. Therefore the PL of PEI-QDs was quenched as the incubation time increased and then approached a constant value after 2 h (Figure 4B). Finally, 2 h was selected as the incubation time for the fluorescent detection. In addition, PEI-QDs showed no obvious PL decline to thrombin except for the slight blue shift of emission wavelength (Figure S6, Supporting Information).

Fluorescent Detection of Thrombin. Under the optimal assay conditions, PL of PEI-QDs sensitively decreased with the increase of thrombin concentration (Figure 5A). The calibration plot showed a good linear relationship between the fluorescence intensity ratio of F_0/F and the logarithmic value of thrombin concentration in a range of 0.075 to 12.5 μM with a correlation coefficient of 0.993 (inset in Figure 5A). Here, F_0 and F are the fluorescence intensities detected in the absence and presence of target, respectively. The detection limit at 3σ was 67 nM, which was much lower than that of the above UV−vis spectroscopic analysis of 0.46 μM. This method with high sensitivity is promising in practical applications.

Selectivity of DNA Hydrogel. In this experiment, human IgG antibody, BSA, and lysozyme were selected to study the specificity. Little change of PEI-QDs fluorescence was observed for human IgG antibody, BSA, and lysozyme because DNA hydrogel had no gel-to-sol transition with these biological molecules. Meanwhile, a significant fluorescence quenching was observed for thrombin due to the release of AuNPs from the disassembly of DNA hydrogel (Figure 6). The good selectivity

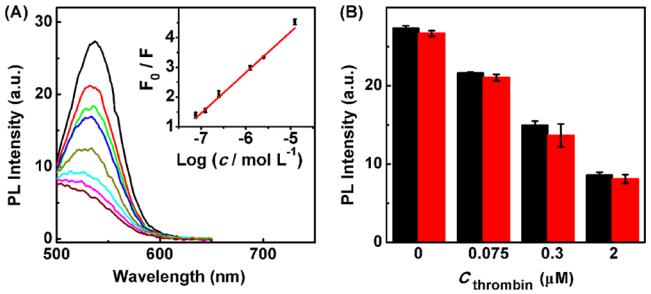

Figure 5. (A) Fluorescence response of this system to thrombin at the concentrations of 0, 0.075, 0.125, 0.25, 1.25, 2.5, 12.5, and 250 μM (from top to bottom). Inset: Calibration curve of PL intensity ratio vs logarithmic value of thrombin concentration. (B) Fluorescent results obtained in serum samples spiked with thrombin (red histograms) and comparison with the same concentrations tested in buffer (black histograms) after incubation with DNA hydrogel.

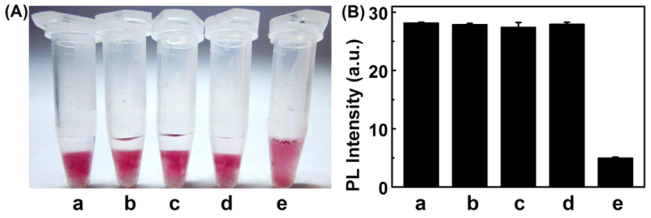

Figure 6. Selectivity evaluation of the self-assembled DNA hydrogel by (A) colorimetric and (B) fluorescent techniques against 0.034 g mL^{-1} human IgG antibody (b), BSA (c), and lysozyme (d), and response to 0.017 g mL^{-1} thrombin (e). (a) The initial DNA hydrogel.

for thrombin is attributed to the high specificity of aptamer. The self-assembled DNA hydrogel could also be applied in highly specific fluorescent detection of other aptamer-based targets.

Application in Complex Matrixes. Complex matrixes such as serum were investigated for the practical application of the hydrogel in fluorescent detection of thrombin. Several standard solutions of thrombin were added to serum to test the performance. Since serum does not contain coagulation factors, the addition of thrombin does not affect the samples. Thrombin was detected in serum diluted 1:100 spiked with thrombin in a concentration range of 0.075−2 μM. Comparison between the results obtained with thrombin in serum and buffer demonstrated that the designed assembled DNA hydrogel system was also workable in complex matrixes (Figure 5B), suggesting the feasibility of the strategy in practice.

■ CONCLUSIONS

The pure DNA hydrogel as a target-responsive switchable material was successfully applied in bioanalysis by using AuNPs and QDs as indicating agents. The DNA hydrogel was designed with Y-shaped DNA and aptamer linker through simple DNA self-assembly without DNA−polymer hybrid, resulting in advantages such as biocompatibility, controllability, and ease of synthesis and modification. The DNA alone hydrogel was, for the first time, applied to bioanalysis with the entrapped AuNPs as an indicating agent for visual detection, and exhibited high specificity and stability. Furthermore, based on the excellent FRET inhibition of oppositely charged nanoparticles between PEI-QDs and AuNPs, a more sensitive strategy was achieved for the detection of protein than the visual analysis. The hydrogel method was also workable in complex sample. It

dx.doi.org/10.1021/ac4027725 | Anal. Chem. 2013, 85, 11077−11082

is expected that the DNA hydrogel as a target responsive structure could be designed as a simple, portable, and low-cost device in biosensing.

■ ASSOCIATED CONTENT

Supporting Information

UV−vis absorption spectral response of the assembled DNA hydrogel to thrombin and calibration curve of absorbance vs logarithmic value of thrombin concentration (Figure S1), UV−vis spectrum and TEM image of AuNPs (Figure S2), particle size distribution of MPA-QDs and PEI-QDs suspended in aqueous solution (Figure S3), ζ potential of MPA-QDs and PEI-QDs (Figure S4), dependence of fluorescence quenching efficiency for PEI-QDs on different volumes of AuNPs and photograph of hydrogels loaded with AuNPs at different volumes (Figure S5), and fluorescence spectra of PEI-QDs in the absence and presence of 0.5 mM thrombin (Figure S6). This material is available free of charge via the Internet at http://pubs.acs.org.

■ AUTHOR INFORMATION

Corresponding Author

*Phone/Fax: +86-25-83593593. E-mail: jpl@nju.edu.cn.

Notes

The authors declare no competing financial interest.

■ ACKNOWLEDGMENTS

This work was financially supported by the National Basic Research Program of China (2010CB732400), National Natural Science Foundation of China (21075060, 21135002, 21121091), and the program for New Century Excellent Talents in University (NCET100479).

■ REFERENCES

(1) Hoffman, A. S. *Adv. Drug Delivery Rev.* **2002**, *54*, 3−12.
(2) Kang, H.; Trondoli, A. C.; Zhu, G.; Chen, Y.; Chang, Y. J.; Liu, H.; Huang, Y. F.; Zhang, X.; Tan, W. H. *ACS Nano* **2011**, *5*, 5094−5099.
(3) Hendrickson, G. R.; Smith, M. H.; South, A. B.; Lyon, L. A. *Adv. Funct. Mater.* **2010**, *20*, 1697−1712.
(4) Calvert, P. *Adv. Mater.* **2009**, *21*, 743−756.
(5) Rejinold, S. N.; Chennazhi, K. P.; Tamura, H.; Nair, S. V.; Jayakumar, R. *ACS Appl. Mater. Interfaces* **2011**, *3*, 3654−3665.
(6) Miyata, T.; Jige, M.; Nakaminami, T.; Uragami, T. *Proc. Natl. Acad. Sci. U.S.A.* **2006**, *103*, 1190−1193.
(7) Petka, W. A.; Harden, J. L.; McGrath, K. P.; Wirtz, D.; Tirrell, D. A. *Science* **1998**, *281*, 389−392.
(8) Osada, Y.; Okuzaki, H.; Hori, H. *Nature* **1992**, *355*, 242−244.
(9) Miyata, T.; Asami, N.; Uragami, T. *Nature* **1999**, *399*, 766−769.
(10) Liu, J. W. *Soft Matter* **2011**, *7*, 6757−6767.
(11) Lin, H. X.; Zou, Y.; Huang, Y. S.; Chen, J.; Zhang, W. Y.; Zhuang, Z.; Jenkins, G.; Yang, C. J. *Chem. Commun.* **2011**, *47*, 9312−9314.
(12) Feldkamp, U.; Sacca, B.; Niemeyer, C. M. *Angew. Chem., Int. Ed.* **2009**, *48*, 5996−6000.
(13) Roh, Y. H.; Ruiz, R. C. H.; Peng, S.; Lee, J. B.; Luo, D. *Chem. Soc. Rev.* **2011**, *40*, 5730−5744.
(14) Liu, D. S.; Cheng, E. J.; Yang, Z. Q. *NPG Asia Mater.* **2011**, *3*, 109−114.
(15) Dave, N.; Chan, M. Y.; Huang, P-J. J.; Smith, B. D.; Liu, J. W. *J. Am. Chem. Soc.* **2010**, *132*, 12668−12673.
(16) Nagahara, S.; Matsuda, T. *Polym. Gels Networks* **1996**, *4*, 111−127.
(17) He, X.; Wei, B.; Mi, Y. *Chem. Commun.* **2010**, *46*, 6308−6310.
(18) Li, S.; Chen, N.; Zhang, Z.; Wang, Y. *Biomaterials* **2013**, *34*, 460−469.
(19) Yang, H. H.; Liu, H. P.; Kang, H. Z.; Tan, W. H. *J. Am. Chem. Soc.* **2008**, *130*, 6320−6321.
(20) Zhu, Z.; Wu, C. C.; Liu, H. P.; Zou, Y.; Zhang, X. L.; Kang, H. Z.; Yang, C. J.; Tan, W. H. *Angew. Chem., Int. Ed.* **2010**, *49*, 1052−1056.
(21) Yan, L.; Zhu, Z.; Zou, Y.; Huang, Y. S.; Liu, D. W.; Jia, S. S.; Xu, D. M.; Wu, M.; Zhou, Y.; Zhou, S.; Yang, C. J. *J. Am. Chem. Soc.* **2013**, *135*, 3748−3751.
(22) Park, N.; Um, S. H.; Funabashi, H.; Xu, J.; Luo, D. *Nat. Mater.* **2009**, *8*, 432−437.
(23) Um, S. H.; Lee, J. B.; Park, N.; Kwon, S. Y.; Umbach, C. C.; Luo, D. *Nat. Mater.* **2006**, *5*, 797−801.
(24) Cheng, E. J.; Xing, Y. Z.; Chen, P.; Yang, Y.; Sun, Y. W.; Zhou, D. J.; Xu, L. J.; Fan, Q. H.; Liu, D. S. *Angew. Chem., Int. Ed.* **2009**, *48*, 7660−7663.
(25) Xing, Z.; Cheng, E. J.; Yang, Y.; Chen, P.; Zhang, T.; Sun, Y. W.; Yang, Z. Q.; Liu, D. S. *Adv. Mater.* **2011**, *23*, 1117−1121.
(26) Gill, R.; Zayats, M.; Willner, I. *Angew. Chem., Int. Ed.* **2008**, *47*, 7602−7625.
(27) Clapp, A. R.; Medintz, I. L.; Mauro, J. M.; Fisher, B. R.; Bawendi, M. G.; Mattoussi, H. *J. Am. Chem. Soc.* **2003**, *126*, 301−310.
(28) Sapsford, K. E.; Berti, L.; Medintz, I. L. *Angew. Chem., Int. Ed.* **2006**, *45*, 4562−4589.
(29) Shi, L.; Rosenzweig, N.; Rosenzweig, Z. *Anal. Chem.* **2007**, *79*, 208−214.
(30) Pons, T.; Medintz, I. L.; Sapsford, K. E.; Higashiya, S.; Grimes, A. F.; English, D. S.; Mattoussi, H. *Nano Lett.* **2007**, *7*, 3157−3164.
(31) Wargnier, R.; Baranov, A. V.; Maslov, V. G.; Stsiapura, V.; Artemyev, M.; Pluot, M.; Sukhanova, A.; Nabiev, I. *Nano Lett.* **2004**, *4*, 451−457.
(32) Oh, E.; Hong, M. Y.; Lee, D.; Nam, S. H.; Yoon, H. C.; Kim, H. S. *J. Am. Chem. Soc.* **2005**, *127*, 3270−3271.
(33) Tang, B.; Cao, L.; Xu, K.; Zhuo, L.; Ge, J.; Li, Q.; Yu, L. *Chem.—Eur. J.* **2008**, *14*, 3637−3644.
(34) Quach, A. D.; Crivat, G.; Tarr, M. A.; Rosenzweig, Z. *J. Am. Chem. Soc.* **2011**, *133*, 2028−2030.
(35) Xiang, Y.; Xie, M.; Bash, R.; Chen, J. J. L.; Wang, J. *Angew. Chem., Int. Ed.* **2007**, *46*, 9054−9056.
(36) Um, S. H.; Lee, J. B.; Kwon, S. Y.; Li, Y.; Luo, D. *Nat. Protoc.* **2006**, *1*, 995−1000.
(37) Storhoff, J. J.; Elghanian, R.; Mucic, R. C.; Mirkin, C. A.; Letsinger, R. L. *J. Am. Chem. Soc.* **1998**, *120*, 1959−1964.
(38) Zhang, H.; Zhou, Z.; Yang, B.; Gao, M. Y. *J. Phys. Chem. B* **2003**, *107*, 8−13.
(39) Zhang, H.; Wang, L.; Xiong, H.; Hu, L.; Yang, B.; Li, W. *Adv. Mater.* **2003**, *15*, 1712−1715.
(40) Yu, W. W.; Qu, L. H.; Guo, W. Z.; Peng, X. G. *Chem. Mater.* **2003**, *15*, 2854−2860.
(41) Wu, B. Y.; Wang, H. F.; Chen, J. T.; Yan, X. P. *J. Am. Chem. Soc.* **2011**, *133*, 686−688.